Relations between Pore Structure Parameters and Their Implications for Characterization of MCM-41 Using Gas Adsorption and X-ray Diffraction

Michal Kruk and Mietek Jaroniec*

Department of Chemistry, Kent State University, Kent, Ohio 44242

Abdelhamid Sayari

Department of Chemical Engineering and CERPIC, Universite Laval Ste-Foy, Quebec, Canada G1K 7P4

Received October 12, 1998. Revised Manuscript Received December 7, 1998

Structural parameters for ordered mesoporous materials are shown to be strongly interrelated as a result of their well-defined structures. Equations for mesoporous materials with hexagonal arrays of uniform pores (e.g., MCM-41 and SBA-15) are presented, which can be used to calculate the pore size, pore wall thickness, and specific surface area on the basis of several quantities, which are easily available from X-ray diffraction and gas adsorption data (i.e., the interplanar spacing, primary mesopore volume, and micropore volume). The influence of assumptions about the pore shape, pore wall density, and the presence of microporosity or disordered nonmesostructured domains on the evaluation of structural parameters is examined. It is suggested that because of very large specific surface areas and primary mesopore volumes for many MCM-41 materials, the existence of extensive disordered domains is not a common feature of MCM-41. Examination of X-ray diffraction (XRD) patterns and nitrogen adsorption isotherms led to a conclusion that a detailed characterization of ordered mesoporous materials requires application of both gas adsorption and XRD, since these techniques provide complementary information. To facilitate a comparison of experimental results from different laboratories, some recommendations are made for the reporting of adsorption data and their application in the calculations of specific surface areas and pore size distributions.

Introduction

Recently, synthesis and application of mesoporous molecular sieves have received a lot of attention. Many of these materials, such as MCM-41,[1] MCM-48,[1] FSM-16,[2] SBA-1,[3] SBA-2,[4] and SBA-15[5] exhibit a remarkable degree of structural ordering, which is manifested in periodicity of their structures and uniformity of their pores. Others have partially[6] or fully disordered[7] porous structures with narrow pore size distributions. MCM-41 with a honeycomb structure of uniform pores has been studied much more extensively than other mesoporous molecular sieves and its structure is relatively well-understood. ^{29}Si NMR,[1,8] IR,[8] and Raman spectroscopy[8] were used to demonstrate that the MCM-41 pore walls exhibit properties highly similar to those of amorphous silica. The pore wall density of MCM-41 was in most cases found to be close to that of amorphous silica[9−11] (i.e., about 2.2 g/cm^3) [12] and, only in a few studies, much higher[13] or much lower[14] values were reported. It was demonstrated that, under the assumption of an amorphous structure of the pore walls, experimental X-ray diffraction (XRD) patterns of MCM-41 or similarly structured FSM-16 can readily be reproduced using proper simulation procedures.[15−18]

* To whom correspondence should be addressed. E-mail: Jaroniec@scorpio.kent.edu. Phone: (330) 672 3790. Fax: (330) 672 3816.

(1) Beck, J. S.; Vartuli, J. C.; Roth, W. J.; Leonowicz, M. E.; Kresge, C. T.; Schmitt, K. D.; Chu, C. T.-W.; Olson, D. H.; Sheppard, E. W.; McCullen, S. B.; Higgins, J. B.; Schlenker, J. L. *J. Am. Chem. Soc.* **1992**, *114*, 10834.

(2) Yanagisawa, T.; Shimizu, T.; Kuroda, K.; Kato, C. *Bull. Chem. Soc. Jpn.* **1990**, *63*, 988.

(3) Huo, Q.; Margolese, D. I.; Ciesla, U.; Demuth, D. G.; Feng, P.; Gier, T. E.; Sieger, P.; Firouzi, A.; Chmelka, B. F.; Shüth, F.; Stucky, G. D. *Chem. Mater.* **1994**, *6*, 1176.

(4) Huo, Q.; Margolese, D. I.; Stucky, G. D. *Chem. Mater.* **1996**, *8*, 1147.

(5) Zhao, D.; Feng, J.; Huo, Q.; Melosh, N.; Fredrickson, G. H.; Chmelka, B. F.; Stucky, G. D. *Science* **1998**, *279*, 548.

(6) Tanev, P. T.; Pinnavaia, T. J. *Science* **1995**, *267*, 865.

(7) Ryoo, R.; Kim, J. M.; Ko, C. H.; Shin, C. H. *J. Phys. Chem.* **1996**, *100*, 17718.

(8) Chen, C.-Y.; Li, H.-X.; Davis, M. E. *Microporous Mater.* **1993**, *2*, 17.

(9) Dabadie, T.; Ayral, A.; Guizard, C.; Cot, L.; Lacan, P. *J. Mater. Chem.* **1996**, *6*, 1789.

(10) Marler, B.; Oberhagemann, U.; Vortmann, S.; Gies, H. *Microporous Mater.* **1996**, *6*, 375.

(11) Sonwane, C. G.; Bhatia, S. K.; Calos, N. *Ind. Eng. Chem. Res.* **1998**, *37*, 2271.

(12) Iler, R. K. *The Chemistry of Silica*; Wiley: New York, 1979.

(13) Maddox, M. W.; Olivier, J. P.; Gubbins, K. E. *Langmuir* **1997**, *13*, 1737.

(14) Edler, K. E.; Reynolds, P. A.; White, J. W.; Cookson, D. *J. Chem. Soc., Faraday Trans.* **1997**, *93*, 199.

(15) Feuston, B. P.; Higgins, J. B. *J. Phys. Chem.* **1994**, *98*, 4459.

(16) Stucky, G. D.; Monnier, A.; Schuth, F.; Huo, Q.; Margolese, D.; Kumar, D.; Krishnamurty, M.; Petroff, P.; Firouzi, A.; Janicke, M.; Chmelka, B. F. *Mol. Cryst. Liq. Cryst.* **1994**, *240*, 187.

10.1021/cm981006e CCC: $18.00
Published on Web 01/20/1999

Moreover, low-pressure nitrogen adsorption measurements indicated similarity between surface properties of MCM-41 and chromatographic-grade amorphous silica gels.[19−21] Transmission electron microscopy (TEM) and XRD[1,8,15,16,18] provided clear evidence that the porous structure of MCM-41 consists of hexagonal arrays of uniform pores. TEM studies also indicated that pores of MCM-41 may exhibit a certain degree of curvature along their main axis.[22] Moreover, TEM imaging of platinum wires deposited inside the MCM-41 pores[23] demonstrated that the pores are straight or curved to some extent, uniformly sized (diameter of about 3 nm), and parallel, and are without branching. Similarly, polymer mesofibers grown inside MCM-41 channels[24] were shown to have diameters of about 2 nm and could be isolated as either single fibers or bundles of fibers, depending on preparation conditions, confirming the lack of connectivity between the MCM-41 pores. The length of these fibers exceeded their diameter by about 3 orders of magnitude. Gas adsorption provided convincing evidence that some MCM-41 materials exhibit remarkably narrow pore size distributions.[19−21,25−27] This method was also used to show that although most MCM-41 materials do not have micropores,[20,21,25−28] certain synthesis methods may afford samples which exhibit detectable microporosity.[29,30]

The presence of large and easily accessible pores in the structure of MCM-41 was additionally confirmed by suitability of these materials as catalysts as well as supports for catalytically active species[31−33] and chemically bonded ligands.[34−37] Thus, MCM-41 materials were shown to be promising catalysts and catalyst supports suitable for carrying out reactions of large molecules, which are often diffusion-limited or impossible to perform in significantly narrower pores of zeolites and other ordered microporous materials.[31−33] Moreover, the occurrence of large pores together with the siliceous nature of MCM-41 pore walls opened wide opportunities for modification of the MCM-41 surface via bonding organosilanes of desirable structures and functionalities.[34−37] Despite the fact that such modifications cause a considerable pore size decrease, especially in the case of the introduction of high coverages of large ligands,[35,37] the pores of the obtained inorganic−organic composites were still accessible for various molecules, which made the obtained materials suitable as catalysts[36] and highly efficient adsorbents for environmental cleanup.[34]

Although it is clear that MCM-41 exhibits hexagonal arrays of uniform and disconnected mesoporous channels with diameters above about 2 nm, there is still some uncertainty about certain details of its structure. First, it is unclear whether the pore cross-section is circular, hexagonal, or intermediate between these two extremes. The circular pore model was adopted by Mobil's researchers who discovered MCM-41[1,15] and later by many other scientists. However, there also is evidence that the pore shape is hexagonal.[18,38] Transmission electron microscopy is a method of choice in determination of the pore shape, but in the case of MCM-41 and similarly structured materials, TEM results were not conclusive, since it was reported that hexagonal pores can be imaged as circular[18] and circular pores can be imaged as hexagonal[39] under certain experimental conditions. The next question about the MCM-41 structure is whether the hexagonal ordering extends over essentially the whole material or there are some disordered domains and, if so, what is their relative abundance. Lamellar constituents were observed by TEM in structures of MCM-41 materials,[18,38] but it was demonstrated that these results may be artifacts caused by misalignment of the specimens and/or by curvature of mesoporous channels of the samples.[22] There is also some uncertainty about the thickness of pore walls of MCM-41. In this case, TEM results also need to be treated with caution since improper defocus during the measurements may lead to severe overestimation of the pore wall thickness.[18,40] Thus, the pore wall thickness of about 1 nm appears to be typical.[8,15,16,19,20] The existence of somewhat thicker pore walls was reported for MCM-41 materials prepared under certain conditions,[29,41,42] but much larger values of the wall thickness, such as 2.6 nm,[43] are rather unlikely.[44] Finally, it is not fully understood whether single pores in the MCM-41 structure exhibit uniform or modulated diameter.[42,45,46] High-quality MCM-41 samples have extremely narrow pore size distributions,

(17) Inagaki, S.; Sakamoto, Y.; Fukushima, Y.; Terasaki, O. *Chem. Mater.* **1996**, *8*, 2089.
(18) Schacht, S.; Janicke, M.; Schuth, F. *Microporous Mesoporous Mater.* **1998**, *22*, 485.
(19) Kruk, M.; Jaroniec, M.; Sayari, A. *J. Phys. Chem. B* **1997**, *101*, 583.
(20) Kruk, M.; Jaroniec, M.; Ryoo, R.; Kim, J. M. *Microporous Mater.* **1997**, *12*, 93.
(21) Kruk, M.; Jaroniec, M.; Sayari, A. *Langmuir* **1997**, *13*, 6267.
(22) Chenite, A.; Le Page, Y.; Sayari, A. *Chem. Mater.* **1995**, *7*, 1015.
(23) Ko, C. H.; Ryoo, R. *Chem. Commun.* **1996**, 2467.
(24) Johnson, S. A.; Khushalani, D.; Coombs, N.; Mallouk, T. E.; Ozin, G. A. *J. Mater. Chem.* **1998**, *8*, 13.
(25) Franke, O.; Schulz-Ekloff, G.; Rathousky, J.; Starek, J.; Zukal, A. *J. Chem. Soc., Chem. Commun.* **1993**, 724.
(26) Branton, P. J.; Hall, P. G.; Sing, K. S. W. *J. Chem. Soc., Chem. Commun.* **1993**, 1257.
(27) Ravikovitch, P. I.; Domhnaill, S. C. O.; Neimark, A. V.; Schüth, F.; Unger, K. K. *Langmuir* **1995**, *11*, 4765.
(28) Ravikovitch, P. I.; Wei, D.; Chueh, W. T.; Haller, G. L.; Neimark, A. V. *J. Phys. Chem. B* **1997**, *101*, 3671.
(29) Sayari, A.; Liu, P.; Kruk, M.; Jaroniec, M. *Chem. Mater.* **1997**, *9*, 2499.
(30) Sayari, A.; Kruk, M.; Jaroniec, M. *Catal. Lett.* **1997**, *49*, 147.
(31) van Bekkum, H.; Kloetstra, K. R. *Stud. Surf. Sci. Catal.* **1998**, *117*, 171.
(32) Corma, A.; Kumar, D. *Stud. Surf. Sci. Catal.* **1998**, *117*, 201.
(33) Vercuruysse, K. A.; Klingeleers, D. M.; Colling, T.; Jacobs, P. A. *Stud. Surf. Sci. Catal.* **1998**, *117*, 469.
(34) Feng, X.; Fryxell, G. E.; Wang, L.-Q.; Kim, A. Y.; Liu J.; Kemner, K. M. *Science* **1997**, *276*, 923.
(35) Brunel, D.; Cauvel, A.; Fajula, F.; DiRenzo, F. *Stud. Surf. Sci. Catal.* **1995**, *97*, 173.
(36) Cauvel, A.; Renard, G.; Brunel, D. *J. Org. Chem.* **1997**, *62*, 749.
(37) Jaroniec, C. P.; Kruk, M.; Jaroniec, M.; Sayari, A. *J. Phys. Chem. B* **1998**, *102*, 5503.
(38) Alfredsson, V.; Keung, M.; Monnier, A.; Stucky, G. D.; Unger, K. K.; Schuth, F. *J. Chem. Soc., Chem. Commun.* **1994**, 921.
(39) Sakamoto, Y.; Inagaki, S.; Ohsuna, T.; Ohnishi, N.; Fukushima, Y.; Nozue, Y.; Terasaki, O. *Microporous Mesoporous Mater.* **1998**, *21*, 589.
(40) Chen, C.-Y.; Xiao, S.-Q.; Davis, M. E. *Microporous Mater.* **1995**, *4*, 1.
(41) Caustel, N.; Di Renzo, F.; Fajula, F. *J. Chem. Soc., Chem. Commun.* **1994**, 967.
(42) Kruk, M.; Jaroniec, M.; Sayari, A. *Microporous Mesoporous Mater.*, in press.
(43) Cheng, C.-F.; Zhou, W.; Park, D. H.; Klinowski, J.; Hargreaves, M.; Gladden, L. F. *J. Chem. Soc., Faraday Trans.* **1997**, *93*, 359.
(44) Ravikovitch, P. I.; Haller, G. L.; Neimark, A. V. *Adv. Colloid Interface Sci.* **1998**, *76−77*, 203.
(45) Stucky, G. D.; Huo, Q.; Firouzi, A.; Chmelka, B. F.; Schacht, S.; Voigt-Martin, I. G.; Schuth, F. *Stud. Surf. Sci. Catal.* **1997**, *105*, 3.
(46) Edler, K. J.; Reynolds, P. A.; White, J. W. *J. Phys. Chem. B* **1998**, *102*, 3676.

which manifests itself in the presence of almost vertical capillary condensation steps on their adsorption isotherms[4,20,26,28,47] and consequently significant variations of the diameter along the pores are improbable. In addition, the feasibility of catalytic reactions for large molecules, the lack of pore blocking after surface modifications with large ligands, and the results of imaging of platinum wires and polymer fibers formed in the structure indicate that pores of MCM-41 usually do not exhibit appreciable modulation.

It was recognized[9,13,19−21,25,30,48−53] that the ordered structure of MCM-41 imposes severe constraints on possible values of its pore structure parameters. First, it was proposed to use relations between the pore volume, specific surface area, and pore diameter for cylindrical or hexagonal pores to reliably estimate the pore size of MCM-41.[25,51] Unfortunately, in this case, surface areas were assessed from nitrogen adsorption at 77 K on the basis of the standard BET method and thus may be expected to be overestimated by 10% or more,[21,49,54] which would lead to a pore size underestimation of the same magnitude. Later, it was recognized that the XRD interplanar spacing and the primary mesopore volume (volume of ordered pores) constitute more reliable parameters for evaluation of the pore size[9,19−21,48−50,52,53] and pore wall thickness[19−21] or even for the estimation of the specific surface area of MCM-41.[9,21,49] The aim of the current study is to examine further the relations between parameters of the MCM-41 structure and to show how assumptions about the pore shape, pore wall density, and the possible presence of disordered nonmesostructured or microporous domains influence the accuracy of characterization of MCM-41 on the basis of experimental gas adsorption and XRD data. In addition, comments about the application of these techniques in studies of mesoporous molecular sieves and recommendations about reporting results derived from gas adsorption measurements are presented.

Experimental Section

Nitrogen adsorption measurements were performed on an ASAP 2010 volumetric adsorption analyzer (Micromeritics, Norcross, GA) as described elsewhere.[19−21] X-ray diffraction spectra were recorded on a Siemens D5000 diffractometer using nickel-filtered Kα radiation. MCM-41 samples A and B were synthesized via a one-step high-temperature (423 K) synthesis procedure similar to that described in ref 55. MCM-41 samples C and D were obtained via postsynthesis restructuring in the emulsion of hexadecyldimethylamine at 343 K for 3 days (sample C) or at 373 K for 6 h (D), as described in detail elsewhere.[56] MCM-41 E was prepared using the postsynthesis restructuring in water for 20 h at 423 K.[42]

Results and Discussion

Calculations of the Pore Size and the Pore Wall Thickness. Recently, simple analytical equations to evaluate the pore diameter of MCM-41 (denoted here as w_d) using the XRD (100) interplanar spacing (denoted as d) and primary mesopore volume (volume of ordered pores; denoted as V_p) were proposed on the basis of geometrical considerations of infinite hexagonal array of uniform pores.[9,19−21,48,49] All of these equations are equivalent and can be expressed as follows:[19−21]

$$w_d = cd\left(\frac{\rho V_p}{1+\rho V_p}\right)^{1/2} \quad (1)$$

where ρ is the density of pore walls and c is a constant, which depends on the pore shape and is equal to 1.213 for circular[19−21,48] and 1.155 for hexagonal pores.[57] The d-spacing is related to the distance between pore centers a in the MCM-41 structure: $a = 2{\cdot}3^{-1/2}d$. The pore size w_d for the hexagonal pore geometry is defined in the current study as the distance between opposite sides of the hexagonal cross-section of the pore, but if one defines it as the diameter of a circle, which has the same area as the hexagonal cross-section, the constant for circular pores ($c = 1.213$) should be used for the hexagonal model.[49] Thus, the apparent difference in pore sizes predicted for these two pore geometries using eq 1 arises from the definitions of the pore diameter. It is also important to note here that the term $\rho V_p/(1 + \rho V_p) = V_p/(1/\rho + V_p)$ is simply the ratio of the primary mesopore volume to the volume of both primary mesopores and pore walls.

Because of the form of eq 1, the accuracy of XRD data is crucial for the evaluation of the pore size, since the latter is directly proportional to the d-spacing. The assessment of the pore size is less dependent on the accuracy of determination of the primary mesopore volume and the pore wall density. Shown in Figures 1 and 2 are (pore diameter)/(pore-center distance) ratios as functions of (i) the primary mesopore volume and (ii) the pore wall density. It can be seen that, except for unrealistically low values of primary mesopore volumes, even large changes in these quantities lead to relatively small changes of the calculated pore diameter. Relative differences in the pore size values calculated using primary mesopore volumes between 0.5 and 1 cm^3/g (i.e., in the range typical for MCM-41) for $\rho = 2.2$ g/cm^3 do not exceed about 15% (see Figure 1). Moreover, relative differences for pore wall densities between 2 and 2.4 g/cm^3 (i.e., within the range expected for amorphous MCM-41 pore walls) are below about 4% (Figure 2). This insensitivity to the density changes makes eq 1 particularly suitable for practical applications since a routine characterization of MCM-41 usually involves XRD studies, which provide the d-spacing as well as

(47) Edler, K. J.; Reynolds, P. A.; Branton, P. J.; Trouw, F. R.; White, J. W. *J. Chem. Soc., Faraday Trans.* **1997**, *93*, 1667.
(48) Romannikov, V. N.; Fenelonov, V. B.; Paukshtis, E. A.; Derevyankin, A. Y.; Zaikovskii, V. I. *Microporous Mesoporous Mater.* **1998**, *21*, 411.
(49) Galarneau, A.; Desplantier, D.; Dutartre, R.; Di Renzo, F. *Microporous Mesoporous Mater.*, in press.
(50) Kruk, M. Ph.D. Dissertation, Kent State University, Kent, OH, 1998.
(51) Ortlam, A.; Rathousky, J.; Schulz-Ekloff, G.; Zukal, A. *Microporous Mater.* **1996**, *6*, 171.
(52) Bhatia, S. K.; Sonwane, C. G. *Langmuir* **1998**, *14*, 1521.
(53) Nguyen, C.; Sonwane, C. G.; Bhatia, S. K.; Do, D. D. *Langmuir* **1998**, *14*, 4950.
(54) Llewellyn, P. L.; Sauerland, C.; Martin, C.; Grillet, Y.; Coulomb, J.-P.; Rouquerol, F.; Rouquerol, J. In *Characterization of Porous Solids IV*; McEnaney, B., Mays, T. J., Rouquerol, J., Rodriguez-Reinoso, F., Sing, K. S. W., Unger, K. K., Eds.; The Royal Society of Chemistry: Cambridge, 1997; p 111.
(55) Kruk, M.; Jaroniec, M.; Sayari, A. *J. Phys. Chem. B*, submitted.
(56) Sayari, A.; Kruk, M.; Jaroniec, M.; Moudrakovski, I. *Adv. Mater.* **1998**, *10*, 1376.
(57) Kruk, M.; Jaroniec, M.; Sayari, A. *Stud. Surf. Sci. Catal.* **1998**, *117*, 325.

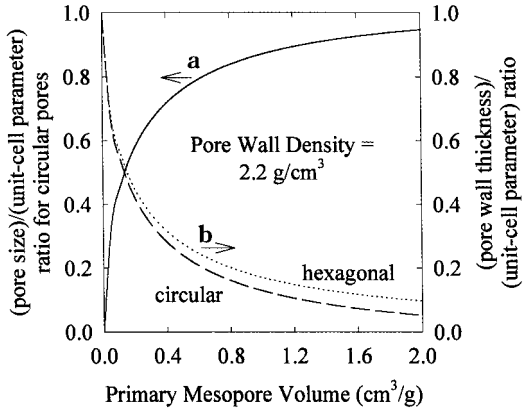

Figure 1. (a) The ratio of the primary mesopore size to the unit-cell parameter (w_d/a) as a function of the primary mesopore volume for the circular pore geometry; (b) the ratio of the pore wall thickness to the unit-cell parameter (b_d/a) as a function of the primary mesopore volume for circular and hexagonal pore geometries. The density of the pore walls was assumed to be 2.2 g/cm^3.

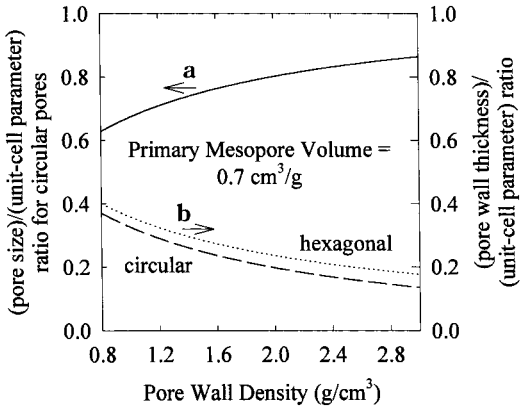

Figure 2. (a) The ratio of the primary mesopore size to the unit-cell parameter (w_d/a) as a function of the pore wall density for the circular pore geometry; (b) the ratio of the pore wall thickness to the unit-cell parameter (b_d/a) as a function of the pore wall density for circular and hexagonal pore geometries. The primary mesopore volume was assumed to be 0.7 cm^3/g.

adsorption measurements, which provide the primary mesopore volume, but often does not involve determination of the pore wall density. Indeed, our work showed[19−21,29,42] that, under the assumption of the MCM-41 pore wall density being equal to that of amorphous silica (2.2 g/cm^3), eq 1 provides results highly consistent with the values of capillary condensation pressures for various MCM-41 materials as well as for FSM-16. The capillary condensation pressure is known to reflect the size of pores present in materials.[58] It is also interesting to note that the relations between capillary condensation/evaporation pressures and the pore size[21] determined using eq 1 confirmed recent predictions based on the density functional theory[27,28] and computer simulations,[13] especially in the region of adsorption−desorption reversibility.

The pore wall thickness for MCM-41 (denoted here as b_d) can also be calculated on the basis of the XRD interplanar spacing and the primary mesopore volume:[19,20]

$$b_d = a - w_d = d\left[\frac{2}{3^{1/2}} - c\left(\frac{\rho V_p}{1+\rho V_p}\right)^{1/2}\right] \qquad (2)$$

where $a = 2\cdot 3^{-1/2} d_{100}$ is the distance between the pore centers in the structure of MCM-41. Equation 2 is very useful since the evaluation of the pore wall thickness for MCM-41 using other techniques is not easy, as was mentioned in the Introduction. For instance, gas adsorption can be used to evaluate the pore diameter from data in the capillary condensation/evaporation pressure region and the obtained pore size can be subtracted from the unit-cell parameter a in order to assess the pore wall thickness. However, such an estimate of the pore size is model-dependent and often very inaccurate,[13,19−21,27,28] unless properly calibrated calculation procedures are used.[21]

As can be seen in Figures 1 and 2, the assumption about the pore geometry (circular vs cylindrical) appreciably influences estimated values of the pore wall thickness (expressed as a ratio between the pore wall thickness b_d and the pore-center distance a, i.e., b_d/a). It should be noted that the pore wall thickness for circular pores provides the width of the thinnest part of the wall, whereas the pore wall thickness for hexagonal pores is uniform. On the basis of eq 2, w_d predicted for the hexagonal model are about 10−30% larger than those predicted for the circular model (depending on particular values of the primary mesopore volume and the pore wall density). For instance, the MCM-41 sample with the pore-center distance of 4 nm and primary mesopore volume in the range 0.5−1.0 cm^3/g is expected to exhibit the pore wall thickness from 0.52 to 0.96 nm for circular pores and from 0.68 to 1.1 nm for hexagonal pores. Despite these differences, both of these models indicate that the pore wall thickness for MCM-41 is considerably smaller than the pore diameter, unless the primary mesopore volume is very small. For instance, the pore wall thickness of 1.5 nm (circular pore, $a = 4$ nm) would lead to V_p of about 0.25 cm^3/g, which is excessively low.

Influence of the Presence of Disordered Domains on the Pore Size Estimation. Equation 1 can be modified to account for the presence of a disordered nonmesostructured phase in the MCM-41 sample. Let us assume that the disordered phase exhibits pores significantly larger than the primary mesopores of MCM-41. In such a case, the primary mesopore volume V_p can be determined on the basis of gas adsorption data using for instance the comparative plot method,[20,25,26,29] but the obtained value actually provides the volume of ordered pores per gram of the sample rather than per gram of the honeycomb structure. If the mass fraction of the hexagonal phase is equal to x ($x \le 1$), the volume of pore walls in the hexagonal phase per gram of the sample will be x/ρ rather than $1/\rho$. Thus, analogous to eq 1, the pore diameter for the ordered part of the MCM-41 material can be expressed as

$$w_d = cd\left(\frac{V_p}{x/\rho + V_p}\right)^{1/2} = cd\left(\frac{\rho V_p}{x + \rho V_p}\right)^{1/2} \qquad (3)$$

It can be seen that eq 3 reduces to eq 1 for $x = 1$ (i.e., when the sample is composed exclusively of the MCM-41 phase). Shown in Figure 3 are (pore size)/(unit-cell

(58) Gregg, S. J.; Sing, K. S. W. *Adsorption, Surface Area and Porosity*; Academic Press: London, 1982.

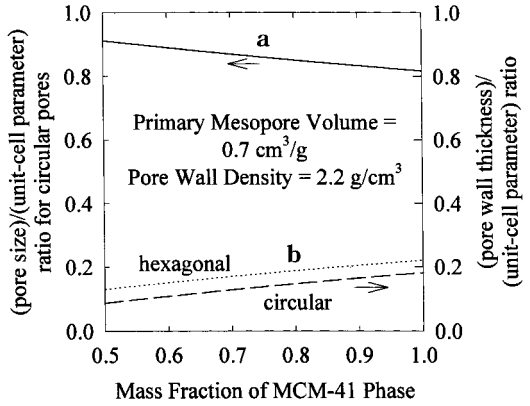

Figure 3. (a) The ratio of the primary mesopore size to the unit-cell parameter (w_d/a) for circular pore geometry as a function of the mass fraction of the MCM-41 phase in the sample with disordered domains; (b) the ratio of the pore wall thickness to the unit-cell parameter (b_d/a) as a function of the mass fraction of the MCM-41 phase in the sample assuming circular and hexagonal pore geometries. The primary mesopore volume and the pore wall density were assumed to be 0.7 cm^3/g and 2.2 g/cm^3, respectively.

parameter) ratios (w_d/a) and (pore wall thickness)/(unit-cell parameter) ratios (b_d/a) as functions of the mass fraction of the MCM-41 phase. One can notice that the application of eq 1 (i.e., eq 3 with $x = 1$) for a partially amorphous MCM-41 sample characterized by $x < 1$ would lead to an underestimation of the primary mesopore size and overestimation of the pore wall thickness for the hexagonally ordered part of the material. It can be expected since the presence of disordered domains lowers the primary mesopore volume and thus suggests a higher volume fraction or equivalently, thickness, of the pore walls, which in turn indicates a lower pore diameter for the material with a given *d*-spacing. As can be seen in Figure 3, the inaccuracy in the pore size evaluation due to the presence of the disordered phase is small, but relative differences in the pore wall thicknesses obtained are much larger. However, it should be noted that the presence of considerable amounts of disordered nonmesostructured phases in MCM-41 samples is usually quite unlikely, since these materials exhibit very high surface areas and pore volumes. For instance, if V_p is equal to 0.7 cm^3/g, the unit-cell parameter is equal to 4 nm and 50% of the mass of the sample would be disordered, one can find that the actual primary mesopore volume for the ordered phase would be 1.4 cm^3/g and the pore wall thickness would be as small as 0.36−0.52 nm (depending on the pore shape), which does not appear to be realistic. Later, it will be shown that considerations of the specific surface area of MCM-41 lead to similar conclusions. Thus, it can be expected that MCM-41 materials with appreciable amounts of amorphous impurities would exhibit low primary mesopore volumes. It is interesting to consider here two MCM-41 materials obtained using a direct synthesis under high-temperature conditions.[55] As can be seen in Figure 4, samples A and B exhibited similar XRD patterns with almost identical *d*-spacings of 5.66 (A) and 5.45 nm (B). As calculated from nitrogen adsorption data,[21] pore sizes of samples A and B are 5.5 and 4.9 nm, respectively (see Figure 5). Primary mesopore volumes for samples A and B are considerably different: 0.97 and 0.29 cm^3/g,

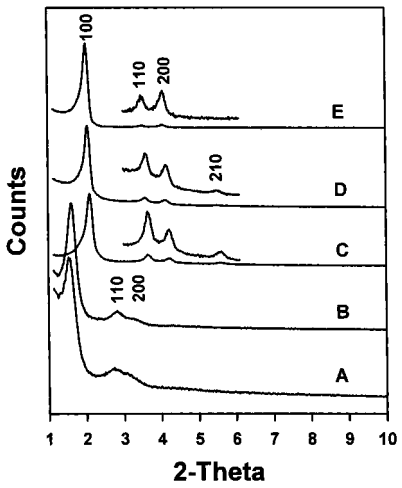

Figure 4. XRD spectra of MCM-41 materials of different degrees of the structural ordering.

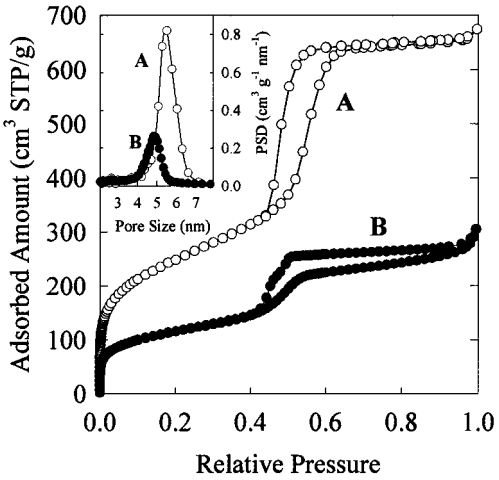

Figure 5. Nitrogen adsorption isotherms and pore size distributions for two MCM-41 materials with similar *d*-spacings. The sample with significantly lower adsorption capacity (B) is expected to have disordered domains.

respectively. The pore size of sample A estimated using eq 1 (i.e., 5.7 nm) is in a good agreement with that obtained using gas adsorption, but eq 1 fails to provide a good estimate of the pore size for sample B, as the value of 4.1 nm is obtained. These results can be explained as follows. Sample A is essentially fully ordered and has a quite typical pore wall thickness (0.9 nm calculated using eq 2). In contrast, sample B has not only thicker pore walls but also a significant amount of amorphous nonmesostructured domains. Since eq 1 does not hold, eq 2 cannot be used to estimate the pore wall thickness for sample B. Instead, one can use the *d*-spacing and the pore size assessed from adsorption data to calculate the pore wall thickness of 1.4 nm, which is quite large. The value of the pore size assessed on the basis of adsorption data (i.e., 4.9 nm) can be explained using eq 3, when one assumes that ≈50% of the mass of sample B constitutes disordered domains. Such a large content of the latter is quite likely since the BET specific surface area and the primary mesopore volume for this sample are exceptionally small (415 m^2/g and 0.29 cm^3/g, respectively). Sample B also exhibits a relatively large external surface area (≈100 m^2/g), which constitutes as much as about 25% of its total surface

area, which is not typical for good-quality MCM-41.[19,20,29] Moreover, one can notice that the shape of the hysteresis loops for samples A and B are markedly different. The hysteresis loop for the former is confined to relative pressures between 0.4 and 0.6 and clearly reflects the irreversibility of adsorption−desorption behavior in primary mesopores. However, in the case of sample B, the hysteresis loop spans from the relative pressure of 0.4 to the saturation vapor pressure and is very pronounced above the pressure range of capillary condensation in primary mesopores (above 0.55), which can be related to the presence of a considerable amount of secondary mesopores. Some of them might be pores between particles of the hexagonally ordered phase, but there is probably an appreciable fraction of secondary mesopores located within disordered domains formed during the synthesis or later as a result of the collapse of the hexagonal phase during the calcination. It can be concluded that disordered domains may indeed be present in some MCM-41 materials, but their occurrence is likely to manifest itself in lower surface areas and mesopore volumes and/or in pronounced broad hysteresis loops on nitrogen adsorption isotherms. On the other hand, XRD data may not provide clear indications of the partially disordered nature of the sample.

Influence of the Presence of Microporosity on the Pore Size Estimation. If a disordered phase present in an MCM-41 sample is microporous, calculations of the primary mesopore volume from adsorption data may be somewhat more difficult, since the micropore volume also would need to be determined,[29,30] but eq 3 is still valid. Thus, the pore size estimated for such a sample using eq 1 would be underestimated. It is also interesting to note that, in the course of our studies of the postsynthesis hydrothermal restructuring of the MCM-41 samples prepared in the presence of octyltrimethylammonium bromide, materials with large *d*-spacings, small primary mesopore sizes, and considerable amounts of micropores were obtained.[30] These anomalous properties were explained on the basis of the assumption that the micropores were located in the pore walls and there was no separate microporous phase. Under these assumptions, the following equation was derived:[30]

$$w_d = cd\left(\frac{V_p}{1/\rho + V_p + V_{mi}}\right)^{1/2} \qquad (4)$$

On the basis of eq 4, it can be inferred that, for a sample, which exhibits certain values of d, V_p, and V_{mi}, the assumption of the presence of microporosity in pore walls leads to smaller primary mesopore sizes and larger pore wall thicknesses than those assessed using eq 1 (i.e., without correction for the micropore volume). In contrast, the assumption about the presence of a separate microporous phase leads to larger primary mesopore sizes and smaller pore wall thicknesses than those calculated on the basis of eq 1. Thus, if an independent estimate of the primary mesopore size (e.g., from gas adsorption data) is available, it may be possible to use geometrical considerations to provide some insight about the location of micropores in the structure of microporous−mesoporous MCM-41 samples. This is potentially very useful in the light of recent attempts to recrystallize pore walls of MCM-41, which may be accompanied with the development of microporosity in the pore wall structure.[59]

Other Relations between Structural Parameters for MCM-41. Equation 2 can be easily rearranged in order to obtain the primary mesopore volume as a function of the interplanar spacing and the pore wall thickness:[50]

$$V_p = \left(\rho\left[\left(\frac{c}{2/3^{1/2} - b_d/d}\right)^2 - 1\right]\right)^{-1} \qquad (5)$$

Likewise, the surface area of primary mesopores S_p can be expressed as a function of some convenient variables, such as V_p and w_d or d and b_d:[21,50]

$$S_p = \frac{4V_p}{w_d} = 4\left(\rho(2/3^{1/2}d - b_d)\left[\left(\frac{c}{2/3^{1/2} - b_d/d}\right)^2 - 1\right]\right)^{-1} \qquad (6)$$

As shown in our previous experimental study,[21] the surface areas of primary mesopores obtained on the basis of the standard BET method[58] (or alternatively, from the α_s-plot method[20,29]) using nitrogen adsorption data are usually 10% or more higher than the values calculated from geometrical considerations using eq 6.[21] The reason for these differences is not fully understood, but may be related to the roughness of the MCM-41 surface or, more likely, to overestimation of the BET specific surface area using a nitrogen adsorbate.[21,49,54] Such an overestimation may result from the incorrect assessment of the monolayer capacity (possibly due to inadequacy of one or more of the assumptions of the BET model, e.g., those about an energetically homogeneous[21] and flat surface) or overestimated value of the cross-sectional area for nitrogen molecules on a silica surface.[49,54] In finding a relation between S_p and S_{BET}, one also needs to keep in mind that MCM-41 samples usually exhibit nonnegligible external surface areas S_{ex} up to about 100−200 m^2/g. Consequently, the experimentally measured nitrogen BET specific surface area for MCM-41 is related to S_p (calculated through eq 6) as follows: $S_{BET} = yS_p + S_{ex}$. Let us assume that y is 1.1 (corresponding to the 10% difference mentioned above) and $S_{ex} = 100$ m^2/g. Using the above relation and the assumed values of y and S_{ex}, one can study the effect of structural parameters, such as d-spacing, pore wall thickness, pore size, and pore volume, on the BET specific surface area. The effect of d-spacing and pore wall thickness on the primary mesopore volume can be examined using eq 5. It can be seen in Figure 6 that, for a constant pore wall thickness (assumed here to be 0.8 nm), the primary mesopore volume increases by a factor of 4 as the d-spacing increases from 2.5 to 10 nm. The corresponding changes in S_{BET} are of a much smaller magnitude, and for d-spacing values above 3 nm, there is a small gradual decrease in S_{BET}. It can be concluded that if MCM-41 materials exhibit similar pore wall thicknesses, large-pore samples would have appreciably higher primary mesopore volumes and only slightly lower surface areas than the samples with typical d-spacings of 3−4 nm. Thus, it is not surprising

(59) Kloetstra, K. R.; van Bekkum, H.; Jansen, J. C. *Chem. Commun.* **1997**, 2281.

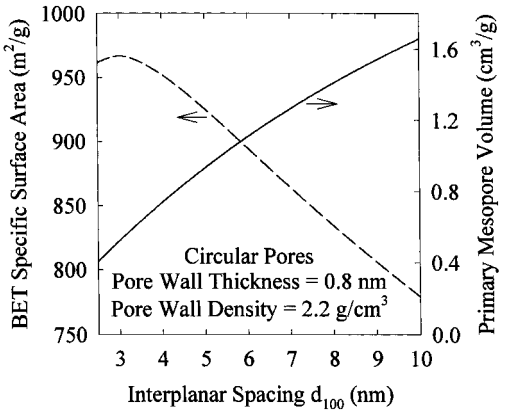

Figure 6. The primary mesopore volume V_p and the BET specific surface area S_{BET} for MCM-41 as functions of the interplanar spacing d_{100} for a constant pore wall thickness of 0.8 nm, assuming the circular pore model.

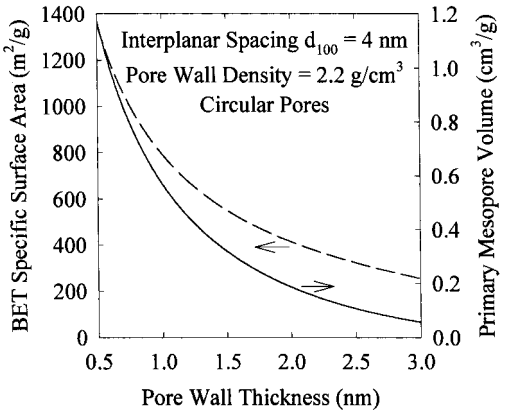

Figure 7. The primary mesopore volume V_p and the BET specific surface area S_{BET} for MCM-41 as functions of the pore wall thickness for a constant interplanar spacing d_{100} of 4.0 nm, assuming the circular pore model.

that the highest values of the primary mesopore volume were reported in the literature for MCM-41 materials with *d*-spacings exceeding 5 nm.[4,56]

It is also interesting to note that an increase in the pore wall thickness of MCM-41 for a constant interplanar spacing value leads to a dramatic lowering in the BET specific surface area and the primary mesopore volume (Figure 7). As was shown in Figure 1, the primary mesopore volume for MCM-41 and similar materials determines the ratio of the pore wall thickness to the unit-cell parameter. Thus, both thick pore walls (above 1.5 nm) and large pore volumes (above 0.5 cm^3/g) can be achieved only for samples with very large *d*-spacings (such as SBA-15[5]).

The presence of a disordered nonmesostructured phase is expected to lead to the lowering of both the primary mesopore volume and BET specific surface area of MCM-41 since usually disordered siliceous materials have much smaller surface areas than ordered mesoporous materials. If a disordered phase constitutes a part of an MCM-41 sample, V_p and S_p values calculated using eqs 5 and 6 would have to be multiplied by the mass fraction of the hexagonal ordered phase in the sample. Thus, an appreciable fraction of disordered domains in the MCM-41 material would significantly lower its primary mesopore surface area and volume. Many MCM-41 materials exhibit an S_{BET} of 1000 m^2/g or more. It can be seen in Figure 7 that such surface areas can be achieved when the pore walls are thin (i.e., about 0.7 nm (for a cylindrical pore model)). If one assumes that a sample with an S_{BET} of about 1000 m^2/g has a significant fraction of disordered domains, the surface area of ordered domains would have to be much higher than 1000 m^2/g, implying very thin walls (see Figure 7), which would probably render the material less stable.[15,20,41] It also needs to be noted that BET specific surface areas significantly larger than 1000 m^2/g, which were reported for some MCM-41 materials, may be markedly overestimated. Possible sources of such unrealistic results were discussed elsewhere.[19−21]

In the context of the considerations presented in the current work, it should be mentioned that a new model of the MCM-41 structure has recently been proposed primarily on the basis of synchrotron XRD data.[14,47] This model assumed that the pore walls of noncalcined and calcined MCM-41 consist of two distinct regions: an internal higher density part and lower density lining of pore walls. Densities of 0.99 and 0.87 g/cm^3 were obtained for higher and lower density regions, respectively, of a calcined highly ordered MCM-41, which led to the conclusion that there is a significant amount of void space in the pore walls. The pore diameter of this MCM-41 material (*d* of about 3.9 nm) was claimed to be as small as 1.4 nm. The proposed model and its implications are in contradiction with essentially all reported data regarding MCM-41 materials. Moreover, its derivation is questionable, since it was based on simulations of XRD diffraction spectra and it was demonstrated by others[15−18] that conventional models of MCM-41 with amorphous pore walls of normal density can be used to accurately reproduce experimentally observed XRD patterns. The authors of the new model have recently acknowledged that their XRD results can also be explained, if one assumes that pore walls of MCM-41 have densities equal to that of amorphous silica, but (i) the structure resembles that of highly defective MCM-48[47] or (ii) the channels are nonintersecting and have smooth walls, whereas the walls or the channel centroids exhibit appreciable displacements with respect to the hexagonal lattice.[46] Similar to the originally proposed two-layer pore wall model,[14,47] these alternative explanations, and the first one in particular, are difficult to be reconciled with a vast amount of experimental data reported in the literature and therefore appear to be unrealistic, especially as these models were proposed to explain the experimental findings about the structure of high-quality MCM-41.[14,46,47]

Recommendations for Adsorption Data Analysis and Reporting. The relations between the pore structure parameters for MCM-41 and other ordered mesoporous materials can be verified if reliable values of these parameters are determined experimentally. Moreover, these relations can be effectively used only if the required parameters are readily available. These two issues point to the need for development of a standard procedure to report adsorption data and derived quantities (e.g., pore volumes, sizes, and size-distributions as well as surface areas, etc.) for ordered mesoporous materials. Such a standardization would allow for an easy and effective comparison of results obtained in

different laboratories. It is recommended to use common adsorbates, such as nitrogen (at 77 K) or argon (at 77 or 87 K) to characterize structural properties of ordered mesoporous materials. Adsorption isotherms constitute a primary source of information about the surface area and porosity, and therefore, reporting adsorption isotherm data (e.g., in graphical form) allows for a simple and model-independent qualitative comparison of properties of porous materials. In most cases, qualitative information is not sufficient and adsorption data need to be used for calculations of the surface area, pore volume distributions, and so forth. In reporting such results, it is essential to specify what method, parameters, and range of data points were used in the calculations. To estimate surface areas of ordered mesoporous materials, application of either the standard BET method[58] or the comparative plot methods[20,25,29] is recommended. Comparative plot methods are also convenient for the detection of microporosity[29,30] and assessment of primary mesopore volume and external surface area for ordered mesoporous materials.[20,25,26,29,30] Macroporous silica gels appear to be suitable as reference adsorbents for silica-based samples.[20,25,26,29,60] Calculations of the surface area using the standard Barrett−Joyner−Halenda (BJH) method[61] and similar approaches[58] are discouraged since the results may be strongly dependent on the form of the Kelvin equation and statistical film thickness used, the choice of adsorption or desorption data, and range of data points.

In the case of good quality MCM-41 materials, the pore diameter and pore wall thickness can conveniently be obtained on the basis of XRD spacing and primary mesopore volume using eqs 1 and 2. A similar formula (eq 4) was also found to be useful in studies of MCM-41 materials with microporosity in pore walls.[30] The primary mesopore size can also be assessed using the Horvath−Kawazoe method[62] or the version of the DFT software developed for porous carbons,[63] but these methods are not expected to be accurate and the pore size distributions obtained may be grossly misleading, for example, indicating the presence of nonexisting microporosity.[30] On the other hand, a careful application of methods based on the Kelvin equation may allow one to obtain meaningful pore size distributions.[21] However, it needs to be remembered that the Kelvin equation underestimates the pore size of mesopores in the range commonly encountered for ordered mesoporous materials (i.e., below ≈7.5 nm) and is not valid in the micropore range.[21,27,58] Moreover, for many adsorbates, such as nitrogen and argon, there is some limiting pressure, for which adsorption−desorption hysteresis loops close[58] and desorption branches are often quite steep when this pressure is approached. Consequently, the pore size distribution calculations based on desorption data often produce maxima at very similar pore size values.[58] For example, the lower closure point of hysteresis loops for nitrogen at 77 K was found to be at a relative pressure of ≈0.4, which happens to be in the pressure range of capillary condensation in primary mesopores of many ordered mesoporous materials.[21,26,27] Therefore, to avoid the presence of artificial maxima on the pore size distributions and other undesirable effects, the use of adsorption branches of isotherms is recommended. Recently, a corrected form of the Kelvin equation for nitrogen adsorption in cylindrical pores and the statistical film thickness curve for silica-based mesoporous materials were reported.[21] These equations were developed using a series of good-quality MCM-41 materials with pore sizes in the range from 2 to 6.5 nm and therefore promise to be especially accurate and useful in studies of ordered mesoporous materials. The corrected Kelvin equation and the statistical film thickness curve can be used in the BJH method or other similar calculation procedures, allowing for accurate assessment of pore size distributions not only for small mesopores typical for ordered mesoporous materials but also in the whole mesopore range.

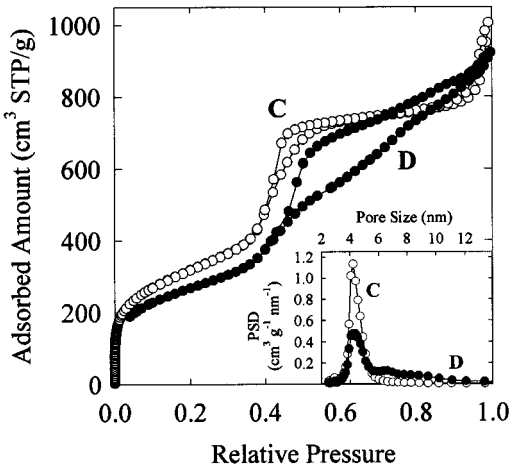

Figure 8. Nitrogen adsorption isotherms and pore size distributions (PSDs) for two MCM-41 materials with similar *d*-spacings and similar positions of the maxima on PSDs, but with significantly different shapes of adsorption isotherms and PSD curves.

Comments on Relations between the Pore Structure of MCM-41 and the Features of Their XRD Spectra. Although the powder X-ray diffraction method is an invaluable tool in determining the symmetry and structure of ordered mesoporous materials, application of this technique as the only source of structural information may be grossly misleading.[64] The XRD technique provides information about the presence of structural ordering in the material studied, but ordered structures may actually constitute only a part of the sample.[18,38,64] For instance, our studies showed that it is possible to synthesize materials which exhibit good XRD patterns characteristic of MCM-41 and yet have very broad pore size distributions. Shown in Figures 4 and 8 are XRD spectra and nitrogen adsorption isotherms for two MCM-41 samples. Both of the adsorption isotherms exhibited capillary condensation steps at relative pressures of about 0.45, which correspond well to their pore sizes expected on the basis of the XRD spacings. In contrast to the adsorption isotherm for the

(60) Kruk, M.; Jaroniec, M. In *Surfaces of Nanoparticles and Porous Materials*; Schwarz, J. A., Contescu, C., Eds.; Marcel Dekker: New York, 1998; p 443.
(61) Barrett, E. P.; Joyner, L. G.; Halenda, P. P. *J. Am. Chem. Soc.* **1951**, *73*, 373.
(62) Horvath, G.; Kawazoe, K. *J. Chem. Eng. Jpn.* **1983**, *16*, 470.
(63) Olivier, J. P. In *Fundamentals in Adsorption*; LeVan, M. D., Ed.; Kluwer: Boston, 1996; p 699.
(64) Ciesla, U.; Grun, M.; Isajeva, T.; Kurganov, A. A.; Neimark, A. V.; Ravikovitch, P.; Schacht, S.; Schuth, F.; Unger, K. K. In *Access in Nanoporous Materials*; Pinnavaia, T. J., Thorpe, M. F., Eds.; Plenum: New York, 1995; p 231.

sample C; the amount adsorbed for sample D steeply increased at relative pressure above 0.55, which reveals an extensive broadening of the pore size distribution (see Figure 8). The presence of larger pores may be responsible for an increased background intensity at very low 2Θ, but otherwise it is difficult to predict from the XRD pattern shown in Figure 4 that sample D has a very broad pore size distribution.

There is also an interesting correlation between the relative intensity of (110) and (200) XRD peaks and the pore wall thickness for ordered mesoporous materials with honeycomb structures. It was already reported on the basis of simulations of XRD patterns of MCM-41[15] that an increase in the thickness of pore walls leads to an increased intensity of the (200) peak with respect to that of the (110) peak. Usually, experimentally observed XRD spectra for MCM-41 exhibit (110) peaks larger than the (200) peaks (see, for instance, XRD spectra for samples A−D shown in Figure 4). One of our MCM-41 materials (sample E) showed a (200) peak that was more pronounced than the (110) peak (see Figure 4).[42] The material exhibited a very low primary mesopore volume (0.46 cm^3/g) and BET specific surface area (600 m^2/g). Using eq 1, the pore size was determined and found to be consistent with the pressure of nitrogen capillary condensation. Thus, on the basis of considerations presented above, the sample was not very likely to be disordered to an appreciable extent and its structural parameters pointed to the presence of very thick pore walls (≈1.5 nm). Similar inversion of intensity of (110) and (200) peaks can be seen on the XRD spectra for SBA-15, which were reported to have thick pore walls in comparison to those for MCM-41.[5] Thus, both simulation and experimental data suggest that the relative intensity of XRD peaks may provide information about the pore wall thickness for certain ordered mesoporous materials.

As was already discussed, adsorption methods provide a significant amount of information about ordered mesoporous materials. However, these methods appear to be insensitive to some details of mesoporous structures (i.e., they do not discriminate between arrays of the pores of different symmetry). For instance, uniform mesopores of hexagonal and disordered arrangements appear to be indistinguishable by very carefully performed nitrogen adsorption experiments.[20] Therefore, in studies of ordered mesoporous materials, it is usually advantageous to use both XRD (to determine the symmetry of the pore structure) and gas adsorption methods (to obtain information about porosity (pore size distribution, pore connectivity, and surface area)).

Acknowledgment. The donors of the Petroleum Research Fund administrated by the American Chemical Society are gratefully acknowledged for support of this research.

Notation

a = distance between pore centers in the hexagonal structure
b_d = pore wall thickness evaluated on the basis of geometrical considerations
c = constant (1.213 for circular and 1.155 for hexagonal pore geometry)
d = XRD (100) interplanar spacing
S_{BET} = BET specific surface area
S_{ex} = external surface area
S_p = specific surface area of primary mesopores evaluated on the basis of geometrical considerations
V_{mi} = micropore volume
V_p = primary mesopore volume
w_d = primary mesopore size evaluated on the basis of geometrical considerations
x = mass fraction of the hexagonal phase in a sample with disordered nonmesostructured domains
y = ratio of primary mesopore surface areas estimated using the BET method and geometrical considerations
ρ = pore wall density

CM981006E